DESY Summer Student Report:

Discovering supersymmetry in the multi-electron channel at ATLAS

Ian Kimpton
University of Oxford
ian.kimpton@lincoln.ox.ac.uk

Supervisor: **Wolfgang Ehrenfeld**

September 15, 2008

Abstract

The ability of the ATLAS detector to discover supersymmetry by studying the topology of the so-called GMSB4 model point is investigated. We study events which produce multiple electrons and make comparisons between predicted Standard Model behaviour and the additional events we should see due to GMSB4. The behaviour of the SUSY and standard model particles is examined, and the potential to measure the relative mass of SUSY particles is briefly discussed.

Contents

1 Introduction

ATLAS is a detector based at the Large Hadron Collider (LHC) in CERN near Geneva, Switzerland. The LHC is a proton-proton particle collider, which will be capable of producing the highest energies yet seen in a particle collider, up to 14 TeV. ATLAS is a general purpose detector, which will be used to probe new physics, which we expect to see due to the high energies the LHC can reach.

This includes looking for the Higgs boson, the only particle in the Standard Model of particle physics yet to be found, as well as looking for evidence of new physics beyond the Standard Model. There are a number of theories for potential new physics beyond the Standard Model, including supersymmetry, string theory and technicolour, but no evidence yet from colliders for physics beyond the Standard Model, so we do not know which, if any, of these theories is correct. However, the Standard Model is currently very successful, with no experiments yet contradicting its predictions, with the exception of the theory of neutrino oscillation, which can be easily accommodated into the theory.

1.1 Standard Model

The Standard Model (SM) of particle physics is a very successful theory, and capable of making very precise predictions which are in agreement with experiment. There are two types of particle in the SM — fermions, which make up matter, and bosons, which carry forces. They all have associated anti-particles (in some cases, particles are their own anti-particles).

The fermions all have spin-$\frac{1}{2}$. They can be subdivided into leptons and quarks. There are three generations of leptons: the (charged) electron, muon and tau, and each of these has an associated (neutral) neutrino. There are six quarks, again in three generations: up, down; charm, strange; top, bottom. The quarks are not found individually, instead they bind to form hadrons, examples of which are the neutron and proton, the building blocks of atomic nuclei.

Three of the four fundamental forces are described by the SM : electromagnetism, weak force and the strong force, but not gravity. The force carriers for all of these are spin-1. The electromagnetic and weak forces have also been unified into one electroweak force. Electromagnetism is carried by the massless photon, while the weak force has 3 massive carriers, the $W^{\pm}$ and the Z^0. The strong force, responsible for holding together quarks is carried by gluons. There are 8 varieties of these, corresponding to different values of colour charge, the strong force's equivalent of electric charge.

The Standard Model also requires the scalar (i.e. spin-0) Higgs particle to ensure that electroweak symmetry is broken (at low energies the EM and weak forces no longer appear unified) and also that particles have mass — without this we have no mechanism for giving any of the particles mass.

1.1.1 Standard Model Successes

As mentioned, the Standard Model of particle physics is a very successful theory. It has achieved unification of the electromagnetic and weak forces, the theories of quantum electrodynamics (QED) and quantum chromodynamics (QCD), which describe the electromagnetic and strong forces respectively, are both elegant and powerful, and can account for all the observed particles and reactions so far. The Standard Model also makes theoretical predictions about parameters, which agree with experiments to very high precision. For example, if we look at the anomalous magnetic moment, $\frac{g_s-2}{2}$ for the electron has agreement between theory and experiment to over 7 significant figures.

1.1.2 Standard Model Problems

The SM is very successful, however it is not thought to be the final theory of physics despite the fact that we have not yet seen it directly contradicted by experiment. To begin with, there are a lot of free parameters in the theory — at least 19 plus those for neutrino oscillations. These must all be measured and put into the theory, they are not predicted by it in any way. The particle masses are free parameters — despite knowing the theory which gives particles masses (Higgs mechanism), we have no idea why some particles are more massive than others. In addition to this, the Higgs theory is yet to be confirmed by experiment — we have not yet observed the Higgs particle.

As mentioned, there are three generations of fermions — but we have no idea why fermions form generations. It also appears to be the case, by looking at the numbers of neutrinos (determined from decay width of Z^0 particle), that there are exactly three generations and not more, and again we have no explanation of this fact.

The theories of electromagnetic and weak forces have been successfully unified, but there are problems in doing this with the strong force. If unification is to occur, we expect the coupling strengths of the forces to all become equal at high enough energies, but this does not happen in the Standard Model. Gravity is also a problem, and there are severe mathematical problems trying to include gravity in the Standard Model framework — it results in non-renormalisable theories, and so the theory breaks down, we have many divergences and infinities appearing in the theory.

Cosmological observations also indicate that of all the energy and matter density in the universe, the standard model particles only contribute 5%. This leaves 95% of the universe unaccounted for — around 25% of this appears to be dark matter, and the remainder appears to be dark energy. These are new forms of matter/energy, and the Standard Model provides no suitable candidates for these.

For these, and other reasons, it is thought that the Standard Model is incomplete, and there are many differing ideas for new physics beyond it, which the LHC will be able to probe by going to very high energies.

2 Supersymmetry

The theory of supersymmetry (often shorted to SUSY) is an extension to the Standard Model. It partners each SM particle with a 'superparticle'. This partner superparticle has the same properties as its SM partner except that it differs by half a unit of spin. Thus all fermions have a superpartner boson and all bosons a superpartner fermion.

The superpartner names are formed by taking the Standard Model particle name, and adding an 's' to the beginning if the Standard Model particle is a fermion, and adding '-ino' to the root if it is a boson. For example, the superpartner to the electron (spin 1/2, charge -1) is the selectron (spin 0, charge -1), and for the photon (spin 1), it is a photino (spin 1/2). The corresponding particle symbols have a tilde added, so the selectron is $\tilde{\mathrm{e}}^-$ and photino is $\tilde{\gamma}$.

2.1 Extra Particles and Complications

In addition to assigning a superpartner to all the SM particles, SUSY theories introduce some additional Higgs particles and their superpartners. In the Standard Model, there is only one Higgs particle. Only a single Higgs doublet is required (this corresponds to four states, since each particle in the doublet has two degrees of freedom), and the three degrees of freedom 'eaten up' by the Ws and Z leaves a single Higgs particle H^0. In SUSY, we require two Higgs doublets to give masses to both up- and down-type particles. This then gives 8 degrees of freedom, 3 of which again are eaten up, and this leaves us with 5 Higgs particles, h^0, H^0, A^0, $H^{\pm}$. In terms of supersymmetric partners to these, the 8 degrees of freedom correspond to 4 spin-$\frac{1}{2}$ Higgsino particles, $\tilde{H}_1^0$, $\tilde{H}_2^0$, $\tilde{H}^{\pm}$.

The graviton, G, a chargeless spin-2 particle responsible for mediating gravity is also introduced in many SUSY theories, and it is possible to construct supersymmetric theories consistent with gravity. Its superpartner, the gravitino $\tilde{\mathrm{G}}$ (spin-3/2) plays an important part in some theories of SUSY, including the GMSB theory, which is the subject of this study.

There are some complications in the superparticles. To begin with, it is not just each particle that the superparticles correspond to, it is each degree of freedom. Since an electron is a spin-$\frac{1}{2}$ particle it has two degrees of a freedom, left-handed and right-handed states. However, a selectron is spin-0 and so has only one degree of freedom. Thus two selectrons are required, one corresponding to the left-handed state and one to the right-handed state. This occurs for all the fermions, expect the neutrinos which only have left-handed states.

This situation is further complicated by the fact that for the third generation of fermions, there is a strong mixing between left- and right-handed states, so instead we have to label the particles by $_{1,2}$ rather than left- and right-handed.

We also get mixing between states with the same quantum numbers, and so rather than getting pure states of the neutral boson counterparts $\tilde{\gamma}$, $\tilde{Z}^0$, $\tilde{H}_1^0$ and $\tilde{H}_2^0$, these all mix to produce the physical states known as neutralinos, $\tilde{\chi}^0_{1,2,3,4}$. The same happens with charged boson counterparts, the $\tilde{W}^{\pm}$ and $\tilde{H}^{\pm}$ mix to give charginos, $\tilde{\chi}^{\pm}_{1,2}$.

2.2 Broken Symmetry and Masses

Supersymmetry does not exist as a perfect symmetry of nature — otherwise we would have expected to have already seen superparticles, as any perfectly supersymmetric theory has particles and sparticles with the same mass. This indicates that supersymmetry is a broken symmetry (spontaneous symmetry breaking), and so the mass of particles and sparticles is no longer the same.

The masses of the SUSY particles are much higher than those of the SM particles, however their exact values depend on which theory is being considered. It will be important later, that the left- and right-handed sparticles of a given fermion will not necessarily have the same mass, this having important effects in the GMSB theory. Once we introduce masses into the theory, it is now the case that a subscript $_1$ indicates the lightest sparticle, with larger numbers corresponding to heavier particles. For example, $\tilde{\chi}_1^0$ is lighter than the $\tilde{\chi}_2^0$.

2.3 R-parity

SUSY introduces a new multiplicative quantum number (conserved in most SUSY theories), known as R-parity. It takes the value +1 for SM particles, and −1 for sparticles. It can be defined by

$$R = (-1)^{2S+3B+L}$$

where S is the particle spin, B the baryon number and L the lepton number. Thus when we have sparticle production in particle colliders, we expect to see two sparticles produced — the R-parity is +1 before, so must be +1 afterwards.

The conservation of R-parity leads to the stability of the lightest supersymmetric particle (LSP), since there is no allowed decay mode — even if standard model particles are lighter, this would violate R-parity. This may have important repercussions for cosmology, discussed in section 2.4.3. The conservation of R-parity also helps ensure the conservation of baryon and lepton number, and without it some SUSY theories predict very fast proton decays, a lot quicker than the current experimental limits.

2.4 Why Supersymmetry?

There are three major reasons why supersymmetry is favoured, and we will now discuss them in turn.

2.4.1 Hierarchy Problem

Supersymmetry solves several (though not all) of the problems associated with the Standard Model. Perhaps the most popular reason for favouring supersymmetry is because it solves what is known as the 'hierarchy problem'. It relates to problems with quadratic divergences in integrals in the SM.

It is simplest to understand this problem and its resolution by considering an analogous problem. We consider a similar problem which occurred with the theory of the electron prior to the introduction of the positron. It is easier to get an intuitive idea of the problem in this case, so it should be a helpful analogy.

A problem with the (then) theory of the electron arose when one considered the effect of the energy of the electron resulting from its electric charge, $\Delta E = \frac{1}{4\pi\epsilon_0}\frac{e^2}{r}$. This increases the energy of the electron, and hence also the mass. We can write this as

$$m_e^{\text{observed}} = m_e^{\text{bare}} + \text{corrections}.$$

where the Coulomb energy is our correction. We know the electron is smaller than 10^{-19} m [10], and at that distance the correction is around 14000 MeV, whereas the observed mass of the electron is 0.511 Mev, so in the calculation we must have a very large bare mass.

In QED, the calculation of this contribution (it corresponds to a photon loop) leads to a quadratically divergent integral. However, this quadratic divergence can be removed by considering a new contribution which arises if we have anti-particles. A virtual electron and positron can be produced by a quantum fluctuation in the electron's EM field, the positron annihilates with the original electron, just leaving the 'new' electron. Calculating the effect of this process removes the quadratic divergence (it cancels the quadratic divergent term exactly) and replaces it with a logarithmic divergence. This can be removed by replacing the infinity limit with the largest mass (energy) cut-off scale — the Planck scale. Thus our corrections are only order of a few percent, rather than the many orders of magnitude we had previously!

Returning to the Higgs hierarchy problem. The particular integrals we are concerned with are quantum loop corrections to the Higgs mass due to heavy fermions [3] (see figure 1). The SM solution is to introduce an energy cut-off at the Planck scale (2.4×10^{18} MeV [9]). However, the Higgs mass (observed) we see is given by

$$m_{h^0}^{\text{observed}} = m_{h^0}^{\text{bare}} + \text{loop corrections}$$

and these loop corrections may 15 or 16 orders of magnitude greater than the observed mass[3], so we need a massive degree of fine tuning between the numbers in this equation in the SM to produce reasonable results. This is undesirable when we are looking for a fundamental physical theory.

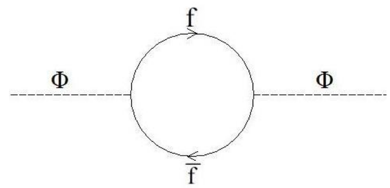

Figure 1: The fermionic loops which contribute to the Higgs mass.

This problem is resolved by SUSY due to its addition of superparticles. This adds additional loops, similar to those before, but with sfermions (which are bosons). Bosonic and fermionic loops have opposite sign, so these loops cancel out the quadratic divergences, resulting only in logarithmic divergences (again renormalisable), so we have no fine tuning problem [9].

SUSY theories also remove even some of the divergences which arise in the SM completely[6], and also have the potential to explain the large difference in energies between electroweak breaking and the Planck mass.

2.4.2 Unification and Gravity

Supersymmetry gives the EM, weak and strong forces the potential to unify. In the SM, the running coupling constants, which indicate the strength for each force, get close to being equal at high energies, but never all meet at one point. However, in SUSY, all three coupling constants

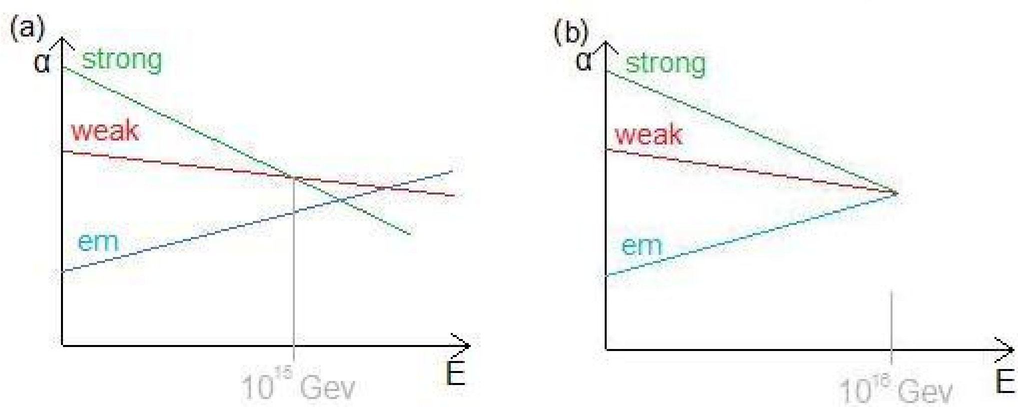

Figure 2: The running coupling constants for the strong, weak and EM forces fail to all meet in the Standard Model (a) but all meet at one point in SUSY (b), allowing unification of these three forces. *Not to scale.*

intersect (figure 2), allowing unification of these three fundamental forces in SUSY theories. This overcomes a potential barrier to constructing what many see as the goal of particle physics — a Grand Unified Theory.

Supersymmetry also allows a renormalisable theory of gravity to be constructed, which is not possible in the Standard Model [5]. This gives us the potential to go one step further than the unification discussed above, and consider possible unification with gravity. In fact, SUSY is an important component of many supergravity and grand unified theories, including string theories [4].

2.4.3 Cosmology

SUSY also may solve problems which arise in cosmology. From observations of the universe, ordinary matter can only account for around 5% of the mass of the universe, with the rest comprising of dark matter and dark energy. The stability of the LSP, due to the conservation of R-parity, means that it is a potential dark matter candidate. Cosmological models of inflation amd SUSY breaking also indicate that there should be a large density of the LSP in the universe[4]. It could thus solve the baffling mystery of why we only know about less than 5% of what makes up the universe!

Cosmological constraints tell us that the LSP must be electrically and colour neutral — otherwise we would have detected exotic effects from the regions with dark matter [4]. In most theories, the LSP is the neutralino $\tilde{\chi}_1^0$, although it is sometimes the gravitino $\tilde{G}$.

2.5 Models of Supersymmetry

There are various models of SUSY, the simplest being the Minimum Supersymmetric Standard Model (MSSM). However, this model's simplicity is not as great as you might expect — it is only minimal in terms of the number of particles. It has 105 unknown parameters [9]. Many consider the arbitrary 19 parameter which the SM has as unsatisfactory, so introducing 105 more is clearly undesirable!

The large number of unknown parameters also makes experimental predictions very difficult. Many theories can improve on this by considering how SUSY is spontaneously broken and these reduce the number of free parameters to a more manageable 5 or 6. They also avoid a potential problem which MSSM has with the mass of the Higgs — it requires a relatively light Higgs to avoid fine tuning problems reappearing [5]. There are several alternatives to the MSSM — Minimal Supergravity (mSUGRA), Gauge-Mediated Supersymmetry Breaking (GMSB) and split-SUSY are some of the more popular.

2.6 GMSB

This report will concentrate on investigating Gauge-Mediated Supersymmetry Breaking. GMSB extends the MSSM by assuming that the symmetry breaking is mediated by the standard model gauge bosons. There are various advantages and disadvantages to this theory — most at a level above this report, but a guide to them is given in sections 3 and 4 of [8]. Unusually in this theory, the LSP is the gravitino rather than a neutralino, and this gravitino can very light [8]. Fortunately, this does not cause problems with either failure to see it, since particles all couple so weakly gravitationally (we have not yet observed gravitons either).

The theory of GMSB has 6 free parameters:

- Λ — the SUSY breaking scale
- $\tan\beta$ — the ratio of the vacuum expectation values of the two Higgs doublets
- N_5 — the number of $SU(5)$ messenger fields
- M_m — the mass of the messenger particles

- sign(μ) — a sign which appears in certain mass shifts
- C_{grav} — related to contributions to the gravitino's mass

The region in GMSB parameter space considered here is known as GMSB4, and these parameters take the values $\Lambda = 30$ TeV, $\tan\beta = 5$, $N_5 = 3$, $M_m = 250$ TeV, sign$(\mu) = +$, $C_{\text{grav}} = 1$.

One important difference between GMSB theories (resulting from different choices of parameters) is what the next-to-lightest supersymmetric particle (NLSP) is. It effects what we are looking for in the ATLAS detector — we cannot see the neutral LSP directly, but can see decay products of the chain which lead to it, as well as the missing energy corresponding to the $\tilde{G}$. In our case, the NLSPs are right-handed sleptons. The right-handed selectron and smuon are assumed to be degenerate in mass, and the stau is only slightly heavier, so all three are nearly degenerate in mass, $m_{\tilde{e}_R} = m_{\tilde{\mu}_R} \approx m_{\tilde{\tau}_1}$, so all act as co-NLSPs.

The full mass spectrum is shown in figure 3. The very light gravitino (2 eV) is not shown —

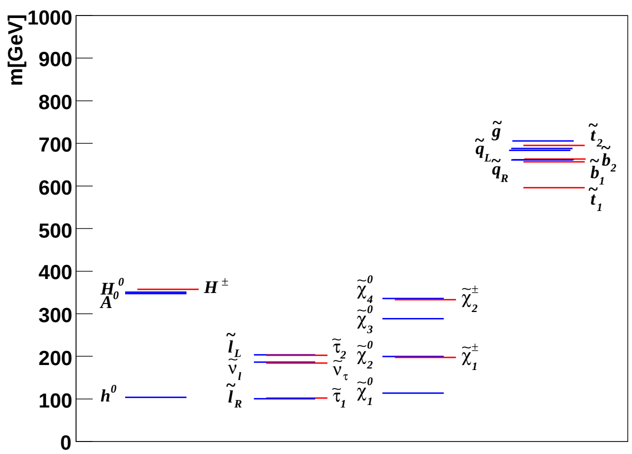

Figure 3: GMSB4 mass spectrum

on this scale it would just appear as 0. The sleptons are clearly the next lightest super-symmetric particles. All the particles above these may decay to the NLSPs (we need more data to know which), however it is most likely that decays where the $\tilde{\chi}_1^0$ acts as the next-to-next-to lightest SUSY particle (NNLSP) in a decay chain will dominate, as this is closest in mass to the sleptons.

We are now in a position to say what sort of signature we expect from a GMSB event. We expect a large amount of missing transverse energy, due to the two undetected gravitons. We also expect to see leptons produced from the end of each of the two SUSY chains present in an event. This is shown in figure 4 for the case of the NLSP being a $\tilde{e}_R$.

So, we expect to see two leptons from the end of each decay branch, and four leptons from these decay chain ends per event (as there are two decay chains of SUSY particles per event). We expect to see an even number of a given flavour of lepton produced from the end of these decay chains — they are always produced in opposite sign but same flavour pairs in the decay $\tilde{\chi}^0 \to \tilde{\ell}_R \ell \to \tilde{G}\ell\ell$ (where ℓ is a general lepton) in order to conserve lepton number.

We have that $\tilde{\chi}^0 \to \tilde{\tau}_R^- \tau^+ \to \tilde{G}\tau^-\tau^+$ or $\tilde{\chi}^0 \to \tilde{\mu}_R^+ \mu^- \to \tilde{G}\mu^+\mu^-$ are allowed, for example, but not $\tilde{\chi}^0 \to \tilde{e}_R^- \mu^+ \to \tilde{G}e^-\mu^+$ or $\tilde{\chi}^0 \to \tilde{e}_R^- e^+ \to \tilde{G}e^+e^+$, since the first violates lepton number and the second violates charge conservation.

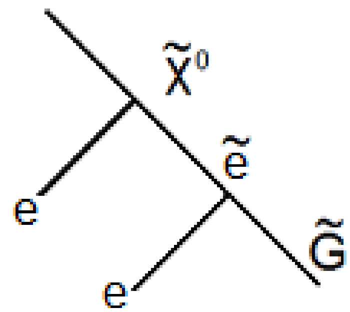

Figure 4: The end of a decay chain where the NLSP is a selectron and the NNLSP a neutralino. Two electrons are produced from this branch.

This all assumes that our NNLSP is always a neutralino (though not necessarily the $\tilde{\chi}^0$). If this assumption is not correct, we expect to see a different collection of products from the end of a decay chain.

Summarising, what we expect to see from our signal events in the detector is:

- A large amount of missing (transverse) energy, corresponding to the gravitinos
- Several leptons produced in each event, 4 of these from the end of the SUSY decay chains

3 LHC and ATLAS

The LHC is a proton-proton collider, based at CERN, with a 27km ring. It can achieve energies of 7 TeV for each proton beam, making a maximum centre-of-mass energy of 14 TeV. There are four experiments based at the ring — ATLAS, ALICE, CMS and LHCb. ATLAS and CMS are general purpose detectors, whereas ALICE and LHCb are more specialised. This study concentrates on ATLAS, the largest of the four detectors, which is shown in figure 5.

3.1 ATLAS

The ATLAS (A Toroidal LHC Apparatus) detector is, as mentioned, a general purpose detector. It is designed to be able to look at all sorts of different physics processes. The structure of ATLAS is very complicated, but it is instructive to look at a simplified picture, shown in figure 6(a). The four major components surrounding the beam pipe in the centre are the central tracker, the EM calorimeter, the hadronic calorimeter and the muon detectors. Other features, such as the magnets, are not shown in this diagram. We will go through each of these components in turn:

- Central tracker — closest to the collision vertex in the beam pipe, this will record charged particles and measure their momentum by looking at their curvature in a magnetic field. Uncharged particles will not be seen.
- EM calorimeter — designed to detect photons and electrons. These interact with the calorimeter, producing showers of alternating Bremsstrahlung photons and pair-produced electrons.

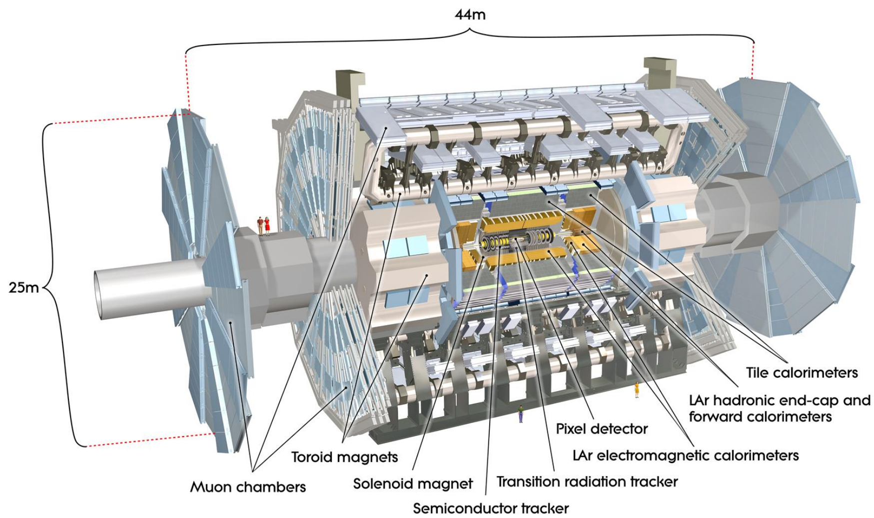

Figure 5: The ATLAS detector (from altas.ch)

Measuring these produced particles enables a determination of the energy. Electrons can be distinguished from photons as they are also seen in the central tracker.

- Hadronic calorimeter — made of very dense material, designed to stop hadronic particles and measure their energy, which they deposit. This stops and measures energy for both neutral and charged hadrons.
- Muon detectors — muons interact less strongly than all the other charged particles in the detector, and so can pass through both calorimeters. There is then a large system on the outside of the detect designed to observe them.

Particles such as neutrinos, or other weakly interacting neutral particles (e.g. our gravitinos) will escape the detector, and can be inferred by looking for missing energy in a collision.

A useful parameter in collisions at ATLAS is the pseudo-rapidity η. This is related to the angle, θ, to the beam direction which a particle follows, as shown in figure 6(b). The relation is given by [7]

$$\eta = -\ln\left[\tan\frac{\theta}{2}\right].$$

This quantity is useful — is is very closely related to the rapidity in Special Relativity, and the pseudo-rapidity between two particles is a relativistic invariant. We also expect particle production to be approximately equal over η[7].

3.2 Proton-proton Colliders

The protons at LHC are accelerated around the ring structure in opposite directions (in different pipes), traversing it many times to enable them to reach very high energies before they collide. It is much easier to accelerate protons than electrons in rings to these sort of energies due to the fact that electrons emit a lot of synchrotron radiation as they go around the bends. This is not as much

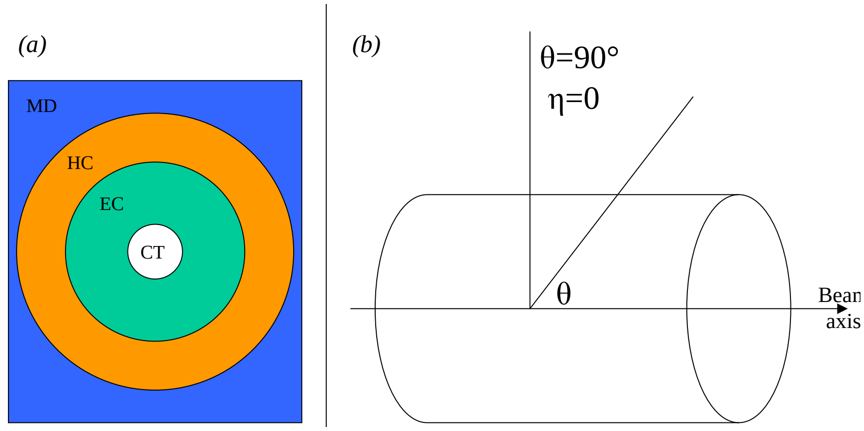

Figure 6: (a) Schematic cut-away of the ATLAS detector, with the central tracker (CT), EM calorimeter (EC), hadronic calorimeter (HC) and muon detectors (MD). *Not to scale.* (b) The angle θ relative to the beam axis.

of a problem for protons, since they are much heavier and the amount of synchrotron radiation emitted goes inversely with mass (actually m^{-4}). This is the main advantage of proton-proton colliders, allowing smaller rings to reach higher energies. Their ability to accelerate is limited by the power of the magnets to make them circulate.

There are, however, some disadvantages to p-p colliders. While they can reach higher energies, a proton-proton event is not as clean as an e^+e^- event. In the latter, you have point-like particle and anti-particle colliding and annihilating, whereas in a proton-proton colliders there is a mixture of partons (constituents of the protons) colliding. Each collision will also not carry the full 14 TeV, as each parton only carries a fraction of the overall proton energy and momentum.

This means that we no longer know the initial state, since it depends on the fraction of momentum and energy carried by each parton. Thus the overall momentum is for the collision is also not known. When we collide the fundamental point-like electrons and positrons, we know that the centre-of-mass frame is the same as the lab frame, but this is no longer the case. Missing or unbalanced momentum is no longer a good indicator for an interesting reaction. However, transverse to the beam direction, we still expect an overall momentum of zero, so we look at transverse momentum, p_T, and the corresponding missing transverse energy (E_T).

3.3 Trigger, Detection and Cuts

In a p-p collision, there may many events occurring simultaneously — if two protons collide, there will be various gluon-gluon, quark-quark, gluon-quark etc. reactions going on just in that collision, making the tracks much more complicated. The proton beams are also large bunches of protons, rather than individual ones, so we expect many protons to be colliding between thee two bunches. Even if we tried to record every event it would simply not be possible to store all the data. There is therefore a trigger system designed to ensure that only events which are 'interesting' or unusual in some way are stored — this is the trigger system.

It is also the case that not every particle will be detected or identified properly. In some cases, this is just due to quantum mechanics underlying the detection interactions, while for others it is related to the geometry of the detector. Since this study will be looking at electrons, we will just consider how this geometry affects them. The specific shape of the EM calorimeters, which we need to see the electrons pass through in order to identify them, means that the value of η must be such that $|\eta| < 2.5$, which means that the trajectory of the electron must deviate by at least 9.4° from the beam direction. This limit results from the geometry of the tracking detector, which is required to find electrons. This helps protect the detector against a lot of the radiation produced in collisions, which occurs very close to the beam direction and would also swamp the detector, making finding these electrons very difficult. Due to the end-caps of the ATLAS detector, there is also a small region at around $|\eta| = 1.4$ where electrons cannot be detected, but our analysis will ignore this as the effect this has will be small.

We also have a limit of minimum transverse energy in order for an electron to be counted. We have more freedom to choose this rather than it being imposed by the geometry, and for this study we require electrons to have at least 15 GeV of transverse momentum. Requiring a high p_T helps ensure that the electron has come from a very high energy interaction, as these are the ones most likely to produce particles with high p_T.

In addition to the trigger cuts, which affect from which events are recorded, we want to make further cuts on events. When performing analyses of data, we do not want to look at all the events the LHC has seen, we want to investigate some subset relevant to our particular investigation. For example, in our GMSB case we expect a high amount of missing transverse energy, so we make some cut on E_T, and only consider events with a high enough value of this. This also helps us reduce our background relative to signal for new physics processes, since we expect overwhelmingly that the reactions undergone in the LHC will be Standard Model processes, and we want to reduce the level to which these dominate over any new physics signal, to enable us to detect these new processes.

3.4 Event Simulation and Generation

While the LHC has not yet begun colliding protons, and so this report cannot use ATLAS data, it is very important that we understand what we may expect to see at the detector before data is taken. This can be done by generating and simulating events. The basis of this is always a Monte Carlo generator, which takes some input data of physics we expect to see and appropriate probabilities, and uses randomly generated numbers to generate physics events. These events may be SM events, or they may be those for new physics. In a typical study, we will want to use both, to enable us to compare the new physics signal with the Standard Model background.

Generating events is very expensive in terms of computing time. Prior to our analysis, two stages are required. First, a Monte Carlo generator must create the raw physics events — all particles, exactly what happens, no detector effects. Secondly, we must then use another Monte Carlo program to simulate what effect the detector has — what we might actually observe from ATLAS after such an event. This processing can take around 10–15 minutes for a single event, so clearly is heavy on computing resources.

Additional software is then required in order to perform appropriate analysis on this to obtain our results. Our analysis was carried out based on SFrame, using C++ and ROOT.

4 Truth Signal Data

For this section of the investigation, we focused on the truth data. This is the information for the generated SUSY events without processing the effect of the detector on the particles. We retain all the information about the origin of particles, and thus decay chains can be reconstructed as we know the parents and the decay products of every particle and can find all particles, even those such as the gravitino or neutrinos which a detector could not see.

It was important to ensure that in our data there were two gravitinos per event. This would provide a useful check of the data sample we were using, and also gave us a starting point to begin constructing the SUSY decay chains. Fortunately, every event contained two gravitinos, as expected. Following this, we began a more detailed study of the SUSY decay chains.

4.1 SUSY Production and Initial Particles

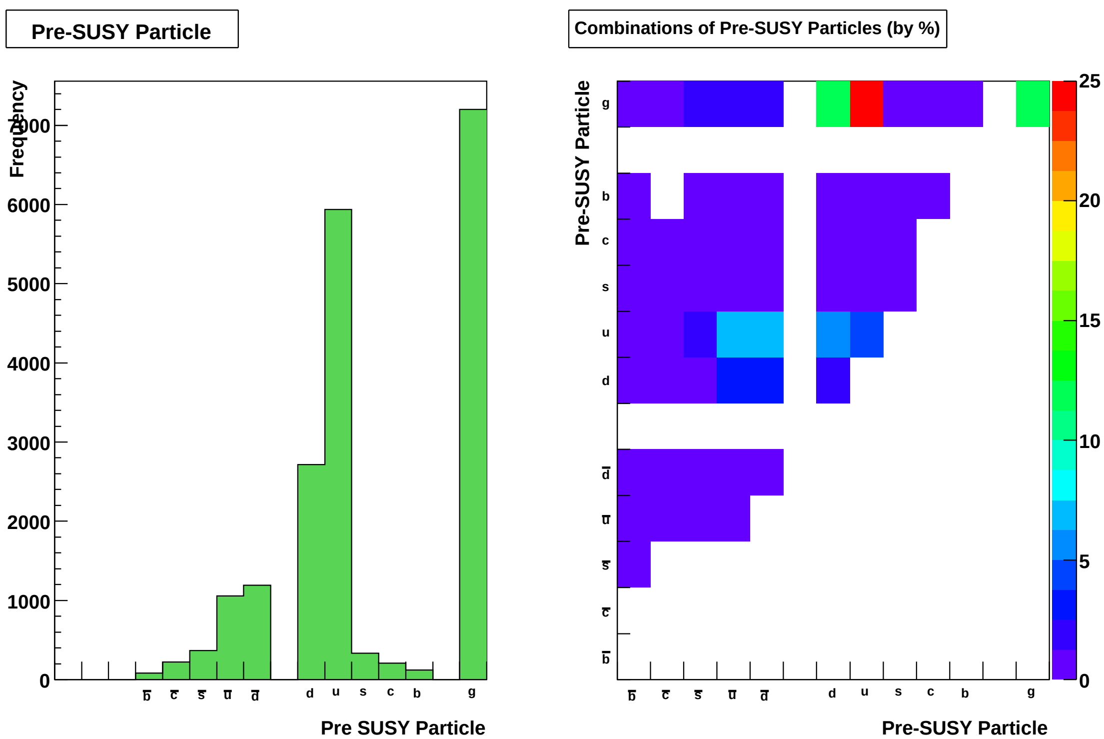

Figure 7: The particles which collide in order to form SUSY particles

The LHC is a proton-proton collider with high energy, and so we mainly expect collisions between gluons and also the valence quarks of the proton (up, down). There will also be a small amount of events containing the other light quarks and anti-quarks, since these can also be found in the proton, but in lower densities so the number of events involving these is reduced. Based on this, the truth data was investigated to see which particles produced the original SUSY particles.

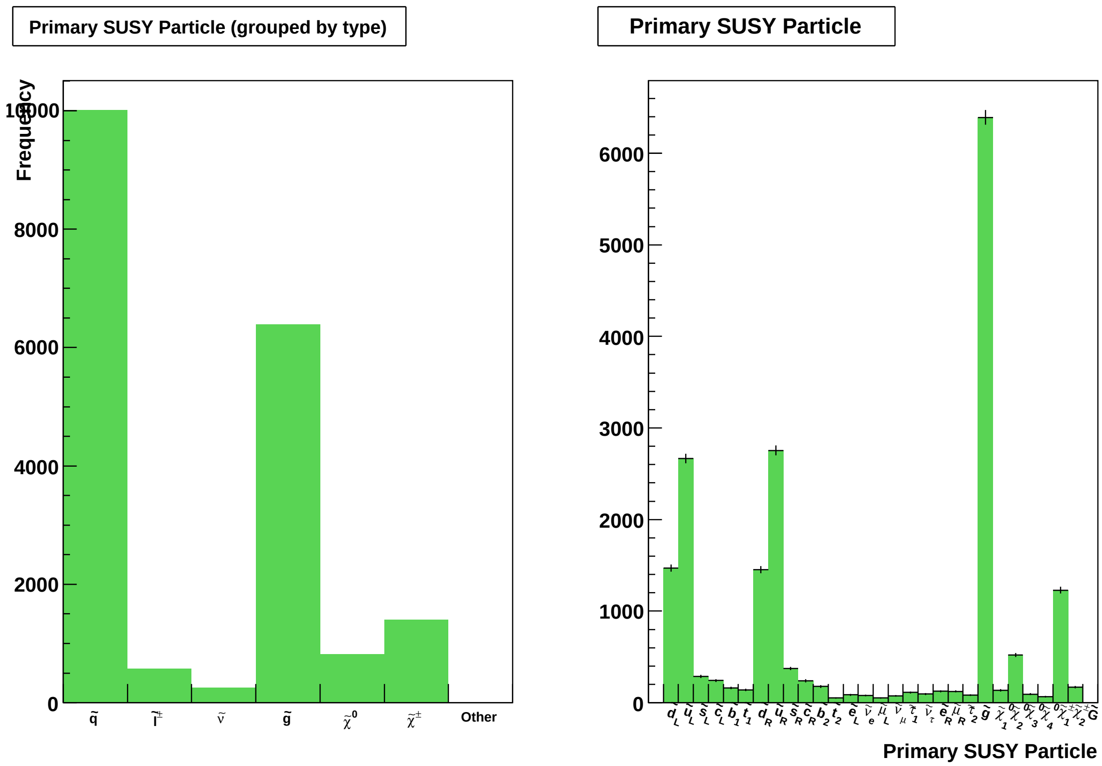

Figure 8: First SUSY particles in chain (particles and anti-particles not shown as distinct). The left hand graph shows the frequency with the SUSY particles categorised, while the right hand graph shows the frequency with which an individual SUSY particle may occur.

Here it became apparent there was a problem with a small subset of the data — 31 out of our 9750 events had no particle prior to the SUSY particles. Further investigation showed that there were also other problems with these events, so they were discarded and not used for analysis beyond this point.

After removing these events, the graphs in figure 7 were produced. They show that the most frequent pre-SUSY particles were indeed the gluons, up quarks and down quarks. The gluons dominate, as we expect for the LHC, and there is roughly a 2:1 ratio of up to down quarks. The expected small contribution of the other light quarks and anti-quarks can be seen. The combinations shown in the right hand side of the figure are also in agreement with what we expect, up quark-gluon being the most likely combination, then gluon-gluon and gluon-down quark. The up quark-gluon dominates over the gluon-gluon case as there are two ways it can occur.

It is thought most likely that the SUSY particles produced in such collisions will be strongly interacting ones, and we again investigated the data to see if this is indeed the case. The results are shown in figure 8. It can seen that the gluinos and squarks dominate, with both the left-handed and right-handed up and down squarks being prominent. This is in agreement with our predictions, since we expect a relationship between these particles and the Standard Model ones which produced them. It is also interesting to note that there are also relatively large contributions from the $\tilde{\chi}_2^0$

and particularly the $\tilde{\chi}_1^{\pm}$ in the remaining cases, higher than even any of the other squarks.

4.2 Search for NLSPs and NNLSPs

Of particular importance in this study is understanding the final steps in the long decay chain. This is where the leptons which give us a signal for GMSB events will be produced. We know already that we expect the NLSPs to be the $\tilde{e}_R$, $\tilde{\mu}_R$ and $\tilde{\tau}_1$ (section 2.6), but we need to investigate whether this is actually the case, and in what proportion they occur. We also suspect that the NNLSP will be a neutralino, most commonly $\tilde{\chi}_1^0$, but again we need to confirm whether this is the case and see if there are any other particles which appear as the NNLSP. Finally, we also need to investigate which standard model particles are produced from the NLSP and NNLSP, and the relative frequencies of these.

4.2.1 NLSPs

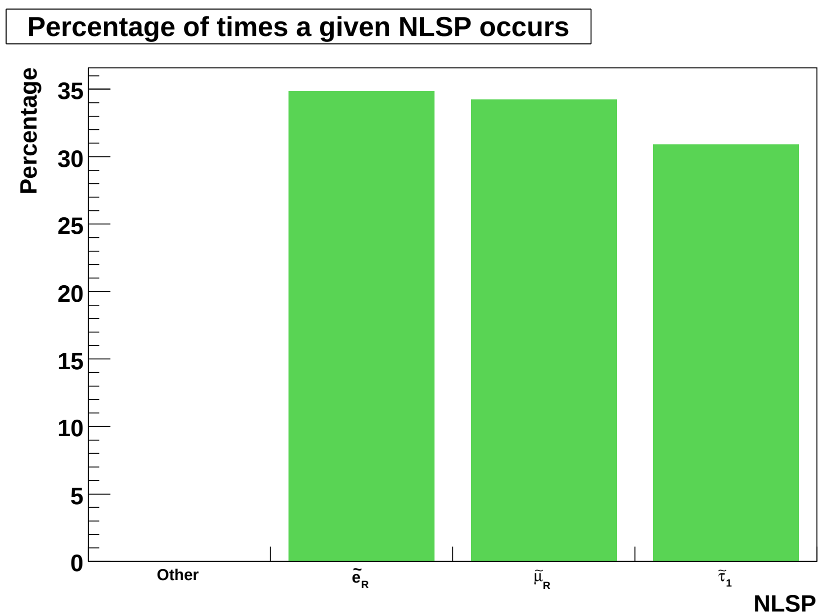

Figure 9: The frequency of which given NLSPs occur.

It is expected that the $\tilde{e}_R$ and $\tilde{\mu}_R$ will be the NLSP in an approximately equal number of cases, as they are assumed degenerate in mass. The $\tilde{\tau}_1$ is slightly heavier so we expect this to occur in a slightly lower but still comparable number of cases. Figure 9 shows the results from analysing the data, and it agrees with this hypothesis. There is a slight over-abundance of selectrons over smuons, but this is very small and likely to just be statistical.

Using this data of how often the individual NLSPs occur, we could calculate how often an event was likely to feature a given combination of NLSPs using simple combinatorics. This could then be compared with the observed numbers. This is done in table 1, and it can be see there is very little deviation — all calculated values are well within 5%, so this indicates there is nothing unusual going on with the pairing of these particles.

Combination	$\tilde{e}_R$, $\tilde{e}_R$	$\tilde{e}_R$, $\tilde{\mu}_R$	$\tilde{e}_R$, $\tilde{\tau}_1$	$\tilde{\mu}_R$, $\tilde{\mu}_R$	$\tilde{\mu}_R$, $\tilde{\tau}_1$	$\tilde{\tau}_1$, $\tilde{\tau}_1$
Calculated	12.1%	23.9%	21.5%	11.7%	21.2%	9.6%
Observed	11.6%	23.3%	21.2%	12.2%	20.8%	9.9%

Table 1: The likelihood of different combinations of NLSP, both calculated and observed.

4.2.2 NNLSPs

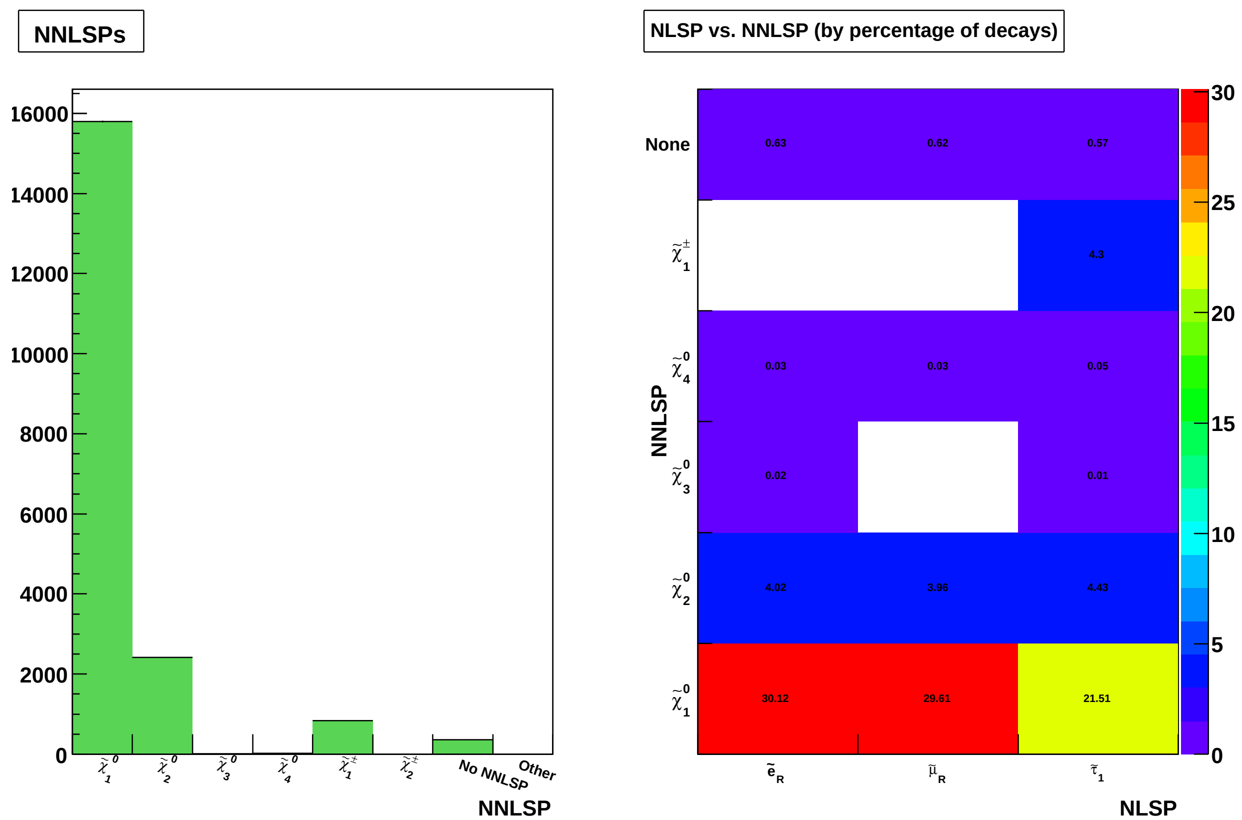

Figure 10: The frequency with which NNLSPs occur, and the frequency of pairings of NLSP & NNLSP.

Now that we understood the NLSPs, we proceeded to investigate the NNLSPs. These are the particles immediately before the NLSP in the SUSY decay chain. What we expected here was less clear than in the NLSP case. While from the mass spectrum (figure 3), we can see that the $\tilde{\chi}_1^0$ can only decay to one of our NLSPs, it was not clear how often other particles would decay directly into the NLSP. Figure 10 shows what occurs in our events.

Over 80% of the time, the NNLSP was indeed the $\tilde{\chi}_1^0$, with the $\tilde{\chi}_2^0$ being next common, occurring 12% of the time. The heavier neutralinos clearly very rarely decay directly to the NLSP. This is all as expected, and will lead to two leptons being produced at the end of each decay branch as in figure 4. However, there are two other cases. One is that there is no NNLSP, and the other that there is a decay to the NLSP from the chargino $\tilde{\chi}_1^{\pm}$.

The first case (no NNLSP) can be easily understood. There is no NNLSP if the first SUSY particle produced is one of the NLSPs. In all but one of the 179 (out of 9719 total events) where this occurred, the originally produced SUSY particles were pairs of NLSPs, e.g. both $\tilde{e}_R$, both $\tilde{\mu}_R$ or both $\tilde{\tau}_1$. In the single other event, the two original particles were $\tilde{\tau}_1$ and $\tilde{\tau}_2$, the second of which then underwent a long decay chain, which culminated in the production of a $\tilde{\mu}_R \to \tilde{G}$, while the other branch just went $\tilde{\tau}_1 \to \tilde{G}$. This occurred only for $\tilde{\tau}$ since the $\tilde{e}_R$ and $\tilde{\mu}_R$ must be produced in pairs to conserve handedness, whereas the $\tilde{\tau}_{1,2}$ are mixtures of handedness states.

The second case is more complicated. It is notable, as mentioned, that figure 10 shows that it only occurs when the NLSP is a $\tilde{\tau}_1$. We now need to understand why this is the case, and we need to look at the chargino to do so. Recall from section 2.1 that the chargino $\tilde{\chi}_1^{\pm}$ results from a mixing between the wino $\tilde{W}^{\pm}$ and the charged Higgsino $\tilde{H}^{\pm}$. Each of these couples either only or much more strongly to the $\tilde{\tau}_1$ rather than $\tilde{e}_R$ or $\tilde{\mu}_R$. The wino only couples to left-handed particles, and so does not couple to the $\tilde{e}_R$ or $\tilde{\mu}_R$, but will couple to the $\tilde{\tau}_1$ as it is a mixture of left- and right-handed states. The Higgsino couples to these particles based on their Standard Model masses, and since the tau is much heavier than the electron or muon, the coupling is much stronger. This all adds up to make the decay from chargino to stau possible, but not for the other sleptons as the coupling is so weak.

4.3 Counting Electrons

4.3.1 Standard Model Products of NLSP and NNLSP

It is important to have an understanding of what the NLSPs and NNLSPs are prior to this section, to understand which standard model particles which result from their decays. The leptons which arise from these two particles decaying are the most important for our signal. As discussed in section 2.6, the main decay we expect is $\cdots \to \tilde{\chi}_1^0 \to \tilde{\ell}\ell \to \ell\ell\tilde{G}$, thus we get two charged leptons and one amount of missing energy (corresponding to the undetected $\tilde{G}$) from each of the two decay branches per event. Thus for a given lepton type, we expect an even number of leptons — either 4 (if the corresponded slepton occurs in both branches), 2 (if it occurs in one branch) or 0 (in neither) leptons.

However, we have seen that it is not only the $\tilde{\chi}_1^0$ which is the NNLSP, nor is it solely one of the other neutralinos (which would give the same decay products) — there are two other, different possibilities. In the case of there being no NNLSP, we expect to see 2 leptons from the whole event (1 from each branch), since we have the decay $\tilde{\ell} \to \ell\tilde{G}$, and the same NLSP occurs on both branches. The single case where we had a $\tilde{\tau}_1$, $\tilde{\tau}_2$ pair produced will have a result from the end of the chain of two muons (the $\tilde{\tau}_2$ happens to decays to $\tilde{\mu}_R$), plus only one τ from the direct decay of the $\tilde{\tau}_1$. Thus we expect at least one event with an odd number of taus.

There was, in addition to the case of no NNLSP, the case where the NNLSP was a chargino, $\tilde{\chi}_1^{\pm}$. In this case, we can't have production of two charged leptons, as this would violate electric charge. So we now expect the decay $\tilde{\chi}_1^{\pm} \to \nu_\ell\tilde{\ell} \to \nu_\ell\ell\tilde{G}$, where the neutrino is required to conserve lepton number. Thus we expected some cases where we observe an odd number of a given type of lepton. Since we know from figure 10 that this decay only occurs for taus, we expect to only see odd numbers of taus rather than electrons or muons. Now knowing what we might expect to observe, we investigated the graphs, shown in figure 11.

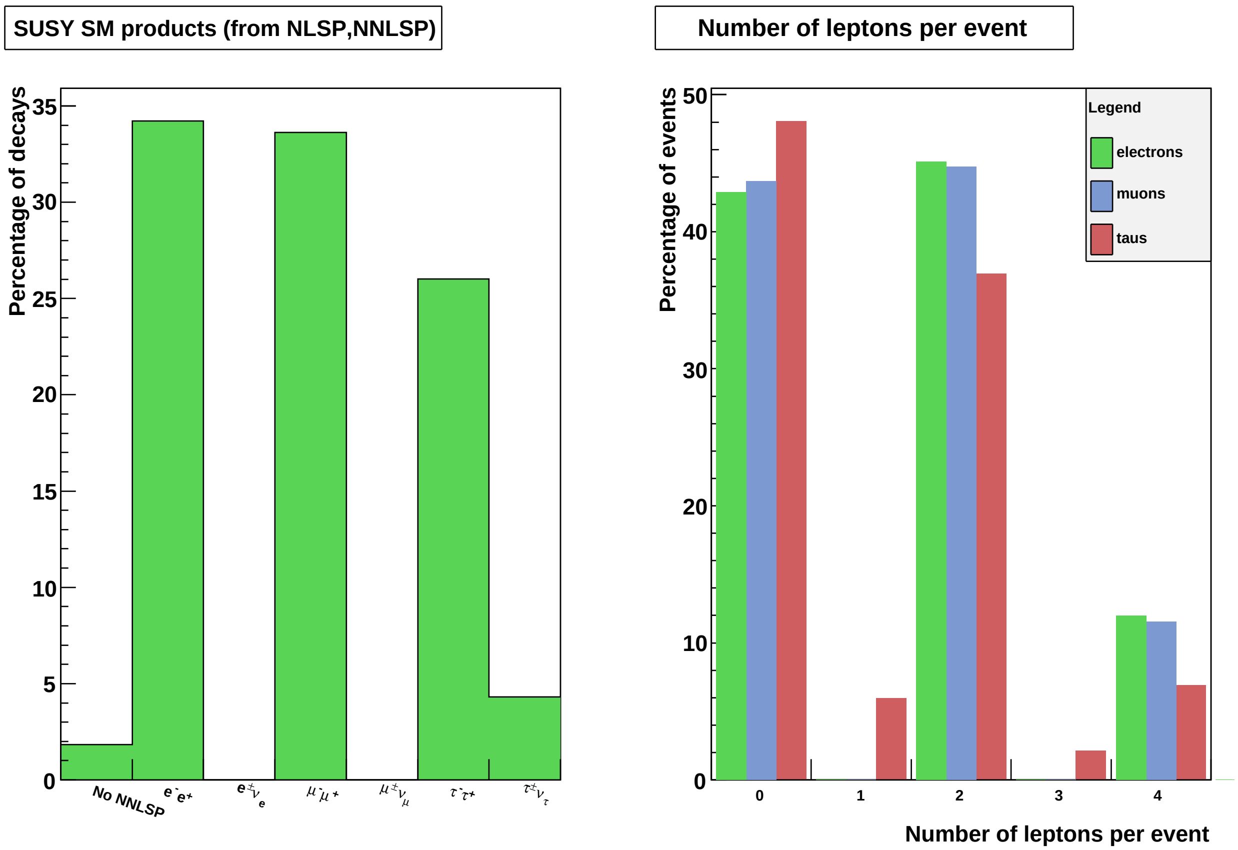

Figure 11: Graphs of the Standard Model products of the decays at the end of the SUSY chain. Left: How often a given decay branch produces a particular lepton combination (No NNLSP only gives one lepton). Right: The numbers of a given type of charged lepton produced per event.

In agreement with our prediction, only odd numbers of taus occur from the end of chains, not electrons or muons. This agrees with our observation that the chargino decay only occurs $\tilde{\tau}_1$ are involved. This is further evidenced by looking at the combinations — $\tau^{\pm}\nu_{\tau}$ occurs, but never $e^{\pm}\nu_e$ or $\mu^{\pm}\nu_{\mu}$. A final cross-check was providing by using the truth data to examine the parents of the produced ν_{τ}, and all cases, the parent was the $\tilde{\chi}_1^{\pm}$.

4.3.2 Counting All Electrons from SUSY

We now know that the very end of the SUSY decay chains always result in an odd number of electrons or muons, but may result in an odd number of taus. It is now worth looking at the lepton count over the whole event. We no longer consider muons or taus from here onwards, as this investigation is mainly focused on electrons. Taus are harder to reconstruct, since they decay in the dectector, and we can only identify them as taus if they undergo a hadronic decay. We will also no longer consider muons, but focus on electrons.

A brief study was made of the number of electrons produced from the whole SUSY chain. These can be seen in the graphs in figure 22 (Appendix A). These are only electrons which came directly from SUSY particles, so any electrons that arose from decays such as $\tilde{\tau}_1^- \rightarrow \tau^- \rightarrow e^-$ will not be included.

The graph clearly shows that the most common value for the number of electrons from SUSY is 2, however 0, 1, 3 and 4 are all around 15% of events, so are clearly not uncommon either, and well over 5% of events include 5 electrons originating directly from SUSY particles. This indicates that the SUSY decay chains in GMSB4 produce a lot of electrons, and so it is a suitable particle to be investigating. However, these counts have been made without any cuts on the events or electron properties, which will reduce the numbers of electrons which are actually observed.

4.4 Electron Origins

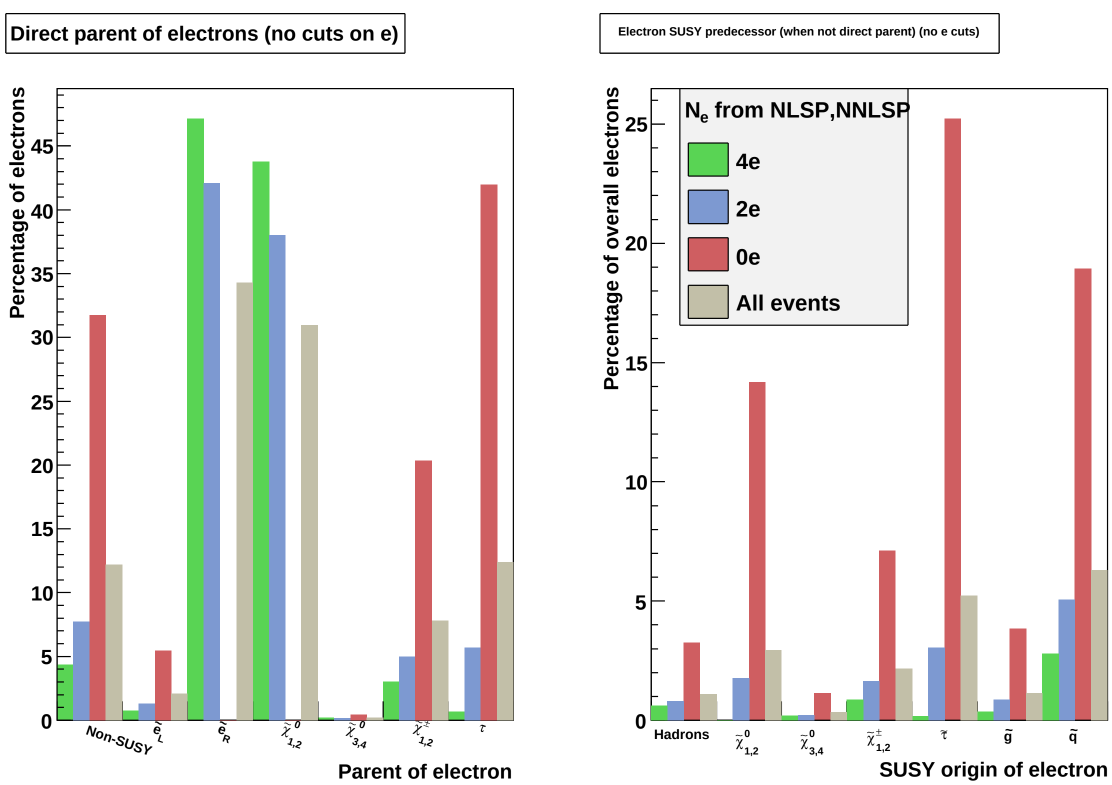

Figure 12: Electron origins — the graph on the left shows the particle which directly produced the electrons. The taus may have a large contribution, so are separated from the other non-SUSY particles. For that case that the parent was non-SUSY (whether τ or otherwise), the graph on the right shows the SUSY origin of the electron.

Having seen how many electrons were produced from SUSY, we now have a look directly at all the electrons in the event, and ascertain the origin of them. We want to know if most electrons are from the end of the SUSY decay chain, from other SUSY decays, or whether they come from other sources. It is also interesting to see how this is affected by the geometric detector and p_T cuts.

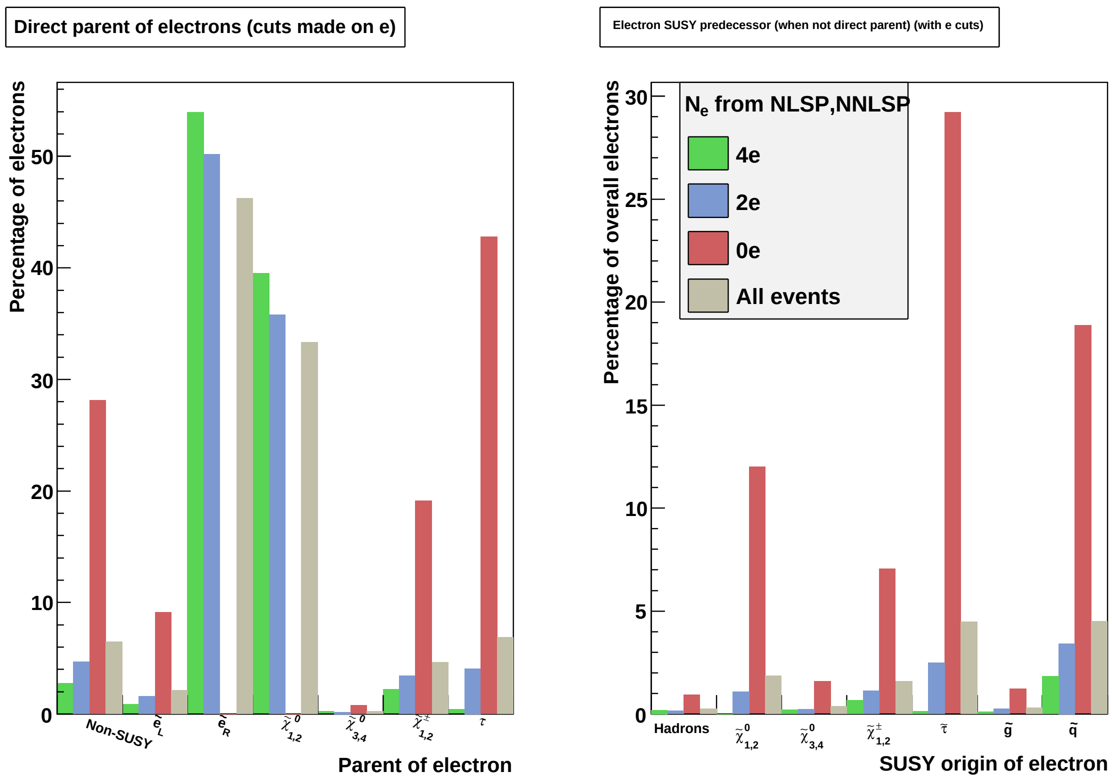

Figure 13: Electron origins as in figure 12, but now with geometric cuts made so only electrons with $|\eta| < 2.5$ and $p_T > 15$ GeV are included.

Graphs were produced for each different case of the number of electrons produced from the NLSP, NNLSP per event. These are shown in figure 12 without cuts and in figure 13 with cuts. There are two graphs for each case — one shows the direct parent of the electron, i.e. the particle whose decay directly produced the electron. The other shows the 'SUSY parent' — the last SUSY particle in the decay chain which led to this electron. For example, in the decay $\tilde{\tau}_1^- \to \tau^- \tilde{G} \to e^-$, the direct parent is the tau, while the SUSY parent of the particle is the $\tilde{\tau}_1^-$.

It is notable that the an overwhelming amount of the electron come from NLSP and NNLSP particles — over 45% come from the $\tilde{e}_R$ once cuts have been made, and well over 30% from the light neutralinos $\tilde{\chi}^0_{1,2}$. In the cases that we have either 4 or 2 electrons produced from the NLSP, NNLSP per event this figure is clearly even greater, and the fact that these cannot produce electrons in the 0 electron case does not significantly reduce the overall fraction of electrons these make up. This is very good news, as it means that it is most likely that electrons from signal events come, as we would like them to, from the NLSP or NNLSPs decaying.

These two are by far the biggest source of electrons. Looking at other sources in the case of cuts, the combined general non-SUSY parent and tau cases add up, in the case of the cuts, to only around 10% of the overall cases, with most of these originating from either $\tilde{\tau}$ or squarks. There are very few electrons seen, particular after we make cuts, which have no SUSY origin whatsoever

Minimum # of electrons	Efficiency
2	76.5%
3	60.4%
4	48.0%

Table 2: The geometric efficiency

(from hadrons). It is also very useful to see that the proporiton of electrons from the NLSP or NNLSP increases after we make cuts, as this is the scenario most like what we observe from the detector.

4.5 Geometric Efficiency

As previously mentioned, we will not see all electrons. One cause of this is the fact that the ATLAS detector will only record electrons with a certain geometry — $|\eta| < 2.5$, $p_T > 15$ GeV, as discussed in section 3.3. We thus used our truth data to produce a geometric efficiency — we compare the number of events with a given number of electrons or more between the cases that we make these cuts and that we don't, *viz*

$$\text{Geometric Efficiency} = \frac{\text{\# of events with more than n electrons (with cuts made)}}{\text{\# of events with more than n electrons (without cuts made)}}$$

By counting the number of electrons in each event, with and without cuts, we were able to produce geometric efficiencies for the cases $n = 2{,}3$ or 4 electrons. Above 4 the statistics are too small, and looking below 2 is not useful as we want to see several electrons in our events. The efficiencies are shown in table 2.

As expected, the efficiency decreases as we increase the minimum number of electrons required from an event. This is not surprising — if we compare requiring at least 4 electrons with requiring at least 2, it is clear that an events with 4 electrons is more likely to lose one electron than an event with 2 — there are more electrons to lose.

This analysis has ignored the region around $\eta = 1.4$ where the detector cannot detect electrons due to the end-caps, however the difference this makes should be minimal.

5 Reconstructed Signal Data

The investigation now moved on to looking at simulated data for our signal events. To obtain these, the truth data is taken and processed by a simulator for the ATLAS detector, mimicking the effects of the detector, and giving an output similar to what we would actually be able to see and determine from the detector.

At this stage, we look at our reconstructed data in three states : before any cuts have been made, after our pre-cuts have been made (to remove certain events), and after electron cuts of $p_T > 15$ GeV and $|\eta| < 2.5$ have been made. The pre-cuts will become important when we look at our background sample later — they are designed to increase the amount of signal events relative to the background. We expect a lot of background, pp collisions produce lots of events, so we need to reduce the total number without losing too many signal events. We achieve this by requiring that we see at least 4 jets, demanding the highest jet $p_T > 100$ GeV and the 2nd, 3rd, 4th have

$p_T > 50$GeV, and also making requiring at least 100 GeV of missing transverse energy. These jet cuts are also motivated by the cuts which have been made on the background sample which we will use.

While this reconstructed data is based on the same number of signal events which we had before, the sample is now weighted so that we have the number of events which we would get once we have obtained 1 fb^{-1} of data. This again will be important when we come to look at the background.

5.1 Electron Distribution

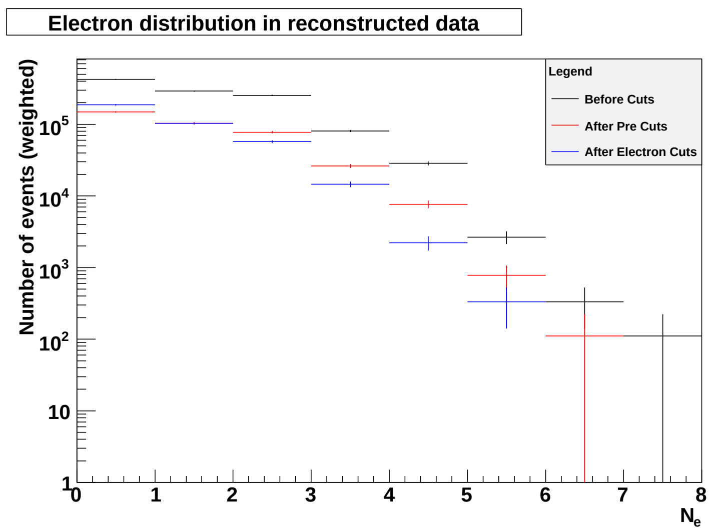

Figure 14: The distribution of number of electrons seen in the reconstructed signal data, before and after our pre-cuts and electron cuts.

We will now have a lower number of electrons than it was in the truth case, as not all electrons will be detected or identified correctly as electrons. We no longer know the source of the electrons, so rather than looking at those produced from just the NLSP, NNLSP or just from SUSY, we look at all electrons, although our truth analysis tells us most electrons will be coming from these SUSY decays. Figure 14 shows the distribution and the effect of our cuts on it. As expected, the events with high numbers of electrons disappear after the electron cuts — these have more electrons, so it is more likely that these will lose at least one in the cuts. The other pre-cuts seems to affect the distribution evenly — the black and red lines on the figure show a similar shape, so our event cuts do not seem to alter the electron distribution very much.

5.2 Missing Transverse Energy

From every event, we expect missing energy of some form due to the two non-interacting gravitinos, however this is not necessarily transverse, and the amount of energy given to the gravitinos varies. We are particularly interested in missing transverse energy, and we make a cut of 100 GeV on it in our pre-cuts. The graph of the missing E_T distribution can be seen in figure 15.

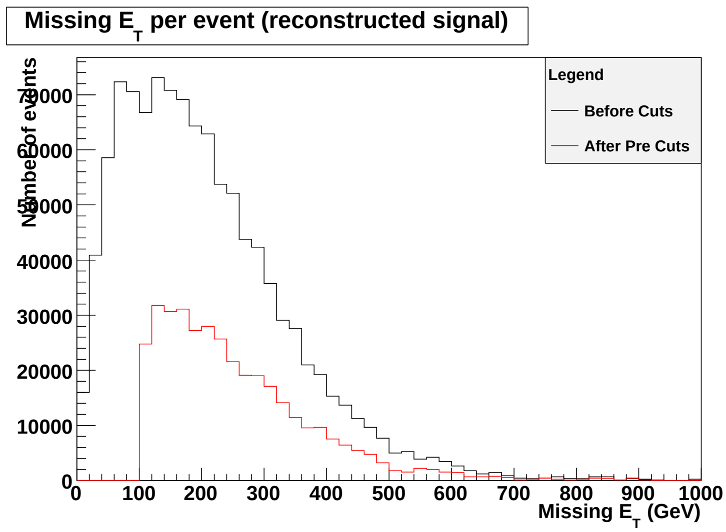

Figure 15: The distribution of missing E_T seen in the reconstructed signal data

Clearly, we had 0 events where the missing $E_T < 100$ GeV after we made the cuts, but other than this the shape of the distribution is the same. It is also interesting that the distribution is flat to around 200 GeV, which indicates it would be possible for us to cut higher on transverse energy without losing too many events.

5.3 Cut Flow

The cuts to the number of events are made progressively, and a record of the number of events left after each cut is saved. The diagram of the cut flow is shown in figure 16. There are 6 cuts on the events as discussed above, determining whether an event is included or not, and then the geometric cuts on the electrons are made — this does not effect the number of events. All but one of the cuts kept above 80% of the previous events, and the cuts on the highest two transverse energy jets kept over 95% of the events. The cut on the transverse momentum of the 4th highest p_T was the only one to reduce our events significantly, to around 64% of what they were prior to the cut. The final missing E_T cut did not reduce the number of events by too large an amount, as expected as we know this model results a decay with at least two particles which will escape detection in every event.

The overall efficiency of ∼35% in these cuts was lower than we get in some other GMSB models. However, these other models have the stau as the sole NLSP, and so taus are produced abundantly. Since tau decays commonly involve jets, it is more than that these high p_T jets will occur. Less stringent cuts on the jets would improve this efficiency, although we cannot decide whether this is worthwhile until we look at our background data.

5.4 Reconstructed Efficiencies

In a similar way to how we calculated our geometric efficiency, we used our electron distribution to calculate a new efficiency. Again, we looked at events with a given number (2,3,4) of electrons

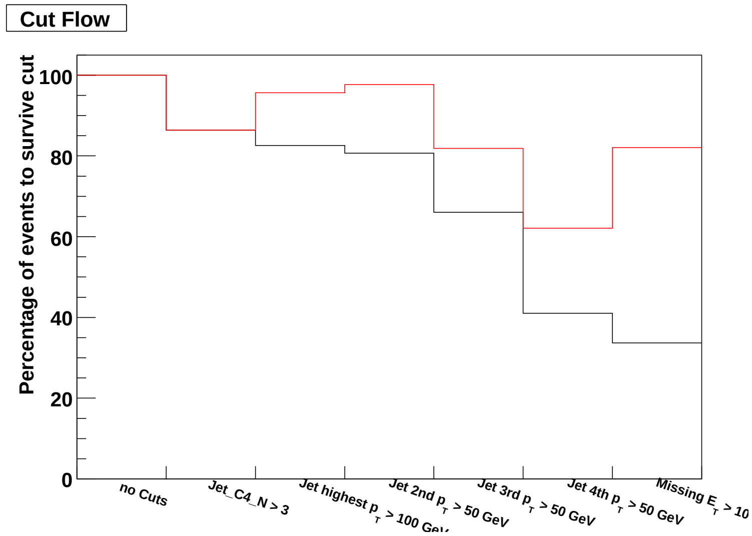

Figure 16: The cut flow diagram for the events in the reconstructed signal data. The black line shows the percentage of events remaining relative to the number we started with; the red line shows the percentage of events remaining relative to the number after the previous cut.

Minimum # of electrons	Efficiency
2	66.3%
3	50.5%
4	31.2%

Table 3: The reconstructed efficiency

or more. By comparing the number of the events in the truth data with those in the reconstructed data (after geometric cuts in both cases)

$$\text{Reconstructed Efficiency} = \frac{\text{\# of events in reco data with more than n electrons}}{\text{\# of events in truth data with more than n electrons}}$$

This efficiency is shown in table 3. It is lower than our geometric efficiency, but not too low.

6 Comparison with Standard Model Background

At the LHC, we will not be able to filter out signal and background events — we don't have 'truth' records for the real data, so we cannot identify 'a' signal event and 'a' background event, we just see the sum of the two (assuming the GMSB4 theory is realised in nature). We therefore need to include some background events in our data, with appropriate cross-sections — they are more likely to occur than SUSY events, but we cannot generate many orders of magnitude higher numbers of events due to the amount of computing time they take.

We carried out investigations with this additional data in much a similar way as with the reconstructed data — we looked at the electron distribution, missing transverse energy and the cut flow. However, now we mostly only deal with the case that all our pre-selection cuts have already been made, as it is only in this case that our background sample is representative. This is because there are some generator cuts on the data — the background already follows certain cuts. This is done to allow our background sample to be representative. If no generator cuts were made, a lot of time would be spent generating non-interesting events that would always be removed by our cuts, and so not feature in our analysis (we cannot simply generate many more events — full simulation takes 10-15 minutes of computing time per event). This would have a knock on effect of increasing the making the statistics of our background sample very poor, since we would still have the same total number of background events, and they would have to be weighted heavily — clearly 100 events weighted by 10 are a better sample and more likely to be representative than 1 event weighted by 1000.

If we compare these generator cuts with our cuts:

- Number of jets - 3 in generator cuts, 4 in pre-selection cuts
- Highest p_T jet - 80 GeV in generator, 100 GeV in pre-selection
- 2nd, 3rd, (4th) p_T jet - 40 GeV in generator, 50 GeV in pre-selection
- Missing E_T - 80 GeV in generator, 100 GeV in pre-selection

Our pre-selection cuts are higher that the generator cuts so we can be sure the generator cuts have no effect on the results, but are close enough to reduce wasted computing time or introducing effects due to poor statistics, as mentioned above.

The generated background came from several areas — Z production, W production, top production and QCD (including $b\bar{b}$) events. As mentioned these background events are weighted, and as in the case of the reconstructed signal data, are based on an integrated luminosity of 1 fb^{-1}.

6.1 Cut Flow

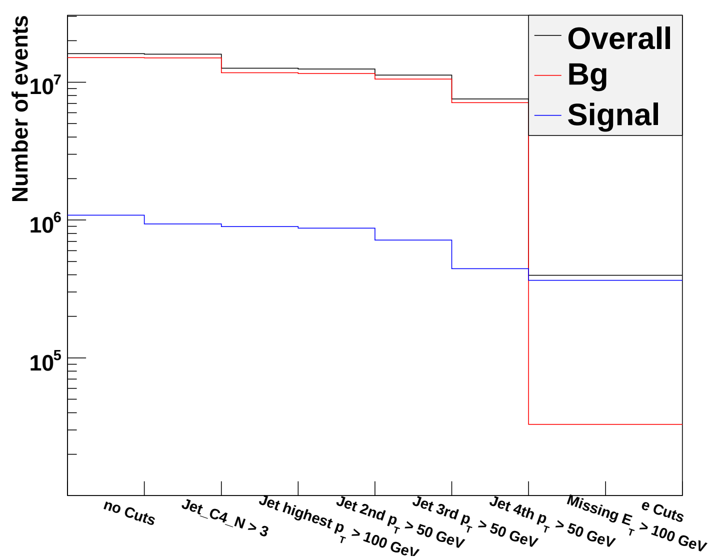

Figure 17: Cut flow

We make the same cuts as in the case of the reconstructed data, and we produce a cut flow diagram, showing all events, signal, and background events in figure 17. As mentioned in above, we have to be careful dealing with the background as this already has some cuts made on it, whereas the signal has none. However, it is clear from this that if we take data with the generator cuts, the only cut of ours which makes a substantial (order of magnitude) difference is the missing E_T cut, and the difference this makes is substantial.

This completely reverses the relative contribution of the signal and background. Prior to this cut, the background had more than an order of magnitude dominance of events over signal, afterwards the signal has well over an order of magnitude dominance over the background. This agrees with what we observed in section 5.2 — it suggests that we could try making even higher missing E_T cuts to increase the dominance of signal over background. It also indicates that of we were to loosen our jet cuts slightly, this would allow us to keep more signal without substantially increasing the background (the jet cuts appear to have very little effect).

We also looked at the cut flow for individual background events, as shown in appendix figure 25. We can see that QCD events always dominate, however they are also the most affected by the missing E_T cut, while the Z, W and top events all reduce by a similar amount to each other.

6.2 Electron Distribution

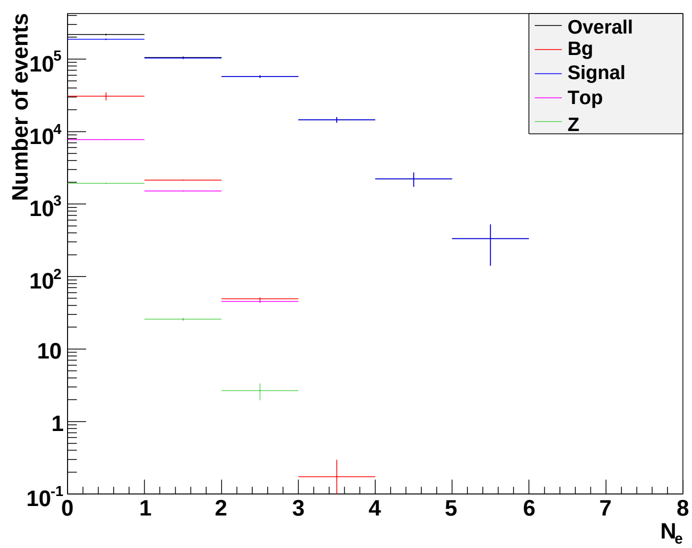

Figure 18: Electron distribution

We looked at the electron distribution after all cuts have been made. Signal events thus dominate over background, and this can be seen in figure 18, and is even more noticeable for high numbers of electrons. Top and Z events are shown for the background since these are most interesting as they produce the highest number of multiple electron events.

A full breakdown of the background electron distribution is figure 23 in the appendix. We can see that while QCD events are most numerous, they very rarely produce electrons. Top and W are the largest contributors by far to the one electron case. Top events produce almost all the cases with two electrons, while top and Z events each give approximately half the three electron events.

6.3 Missing Transverse Energy

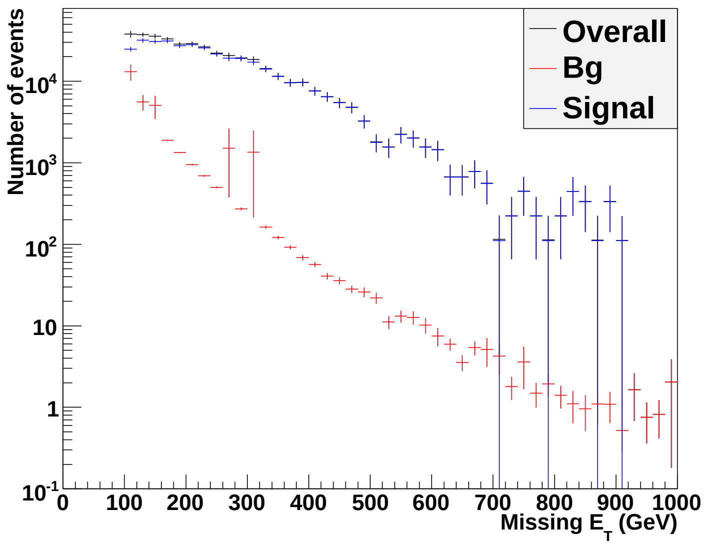

Figure 19: Missing E_T

As in the case of the reconstructed data, we investigated the missing transverse energy spectrum, which can be seen in figure 19, with a comparison of all, signal, and background events. The background has been split up in the appendix figure 24. We see that as we increase the missing E_T, the signal dominance becomes even greater — by 200 GeV the distribution has remained flat, while the background has gone down by an order of magnitude. This again agrees with what have previously seen, and shows that cutting harder on missing E_T (i.e. requiring a higher value) would not affect our signal events too much (which we know from section 5.2. It also shows us that this harder cut on missing E_T will even further decrease our background.

6.4 Significance

Source	Events with at least $\cdots$ electrons						
	0	1	2	3	4	5	6
Z Background	1961	29	2.75	0.09	0	0	0
W Background	5448	584	1.39	0	0	0	0
Top Background	9290	1562	45.32	0.08	0	0	0
QCD Background	16242	17	0	0	0	0	0
All Background	32943	2192	49.45	0.17	0	0	0
Signal	364774	177554	74444	17111.15	2555	333	0
Overall	397717	179746	74493	17111.32	2555	333	0

Table 4: The number of events with a given number of electrons or more.

Using our electron distribution data, we calculated the number of events with a given number or more of electrons, similarly to what we did when calculating efficiencies before. This is shown as a number of events in table 4. Calculating the significance in this case is not helpful, due to the large amount of signal relative to background — we are interested in events with 2 electrons or more, there are ~75000 signal events to 50 background events. From this it is clear that we should see an observable effect from this model of supersymmetry.

7 Relative Mass Determination

Finally, we briefly investigated our ability to determine the relative mass of the $\tilde{\chi}_1^0$ and $\tilde{e}_R$. We can achieve this by looking at so called "opposite sign, same flavour" (OSSF) pairs of leptons — in our case electrons and positrons. The decay from NNLSP to NLSP to the gravitino will, in the case it involves electrons, result in one positron and one electron being produced. If we look at the invariant mass, Δ, of this OSSF pair (i.e. the square root of the sum of the momentum four vectors squared — see equation (7)), we will be able to determine the relative masses of the $\tilde{\chi}_1^0$ and $\tilde{e}_R$. We do this by knowing that the maximum value for this invariant mass in the case we have a decay $\tilde{\chi}_1^0 \to \tilde{e}_R e \to \tilde{G} ee$ is

$$\Delta^2_{\text{max}} = m^2_{\tilde{\chi}_1^0} - - - m^2_{\tilde{e}_R}.$$

This is calculated in Appendix B. We thus look for the corresponding edge in the distribution of the invariant masses of OSSF pairs. Taking $m_{\tilde{\chi}_1^0} = 113.8$ GeV and $m_{\tilde{e}_R} = 100.3$ GeV, we expect the edge at $\Delta = 53.6$ GeV.

7.1 Truth Data

Using truth data, we have the advantage of knowing which particles have been produced from the NLSP, NNLSP. We can thus pair these up and plot the resulting invariant mass, as can be seen in the top left of figure 20. The edge is very well defined in this case, and the few electrons pairs which occur after the edge are from decays where we have had a heavier neutralino decay to the $\tilde{e}_R$. There is no other background, and even this background could be removed by only considering the case the NNLSP is the $\tilde{\chi}_1^0$.

However, we do not have this parent data in real life, so we repeated this process in a more realistic way. We now only use the information of the charge of the particle (to ensure opposite sign pairs) and that it is an electron (to ensure same flavour pairs) to determine our OSSF pairs, but we still use truth data (with no cuts made). All these OSSF pairs were constructed and are plotted, as can be seen in the top right of figure 20. In this case, the edge is still very well defined and is in the same place as previously, indicating a good determination of the invariant mass should be possible. There is now more background due to all the wrongly paired electrons and positrons, however this could be removed in a fuller analysis, since this combinatorial background is approximately constant.

7.2 Reconstructed Data

We then moved on to use reconstructed data, and again we look at the shape of the distribution. This is done after making our pre-cuts on events in the bottom two graphs plotted in figure 20. It is immediately clear that either without (bottom left) or with (bottom right) electron cuts, the peak is still clearly defined. However, now it would definitely be useful to be able to remove the combinatorial background — in the case that we make electron cuts, the edge is only going from

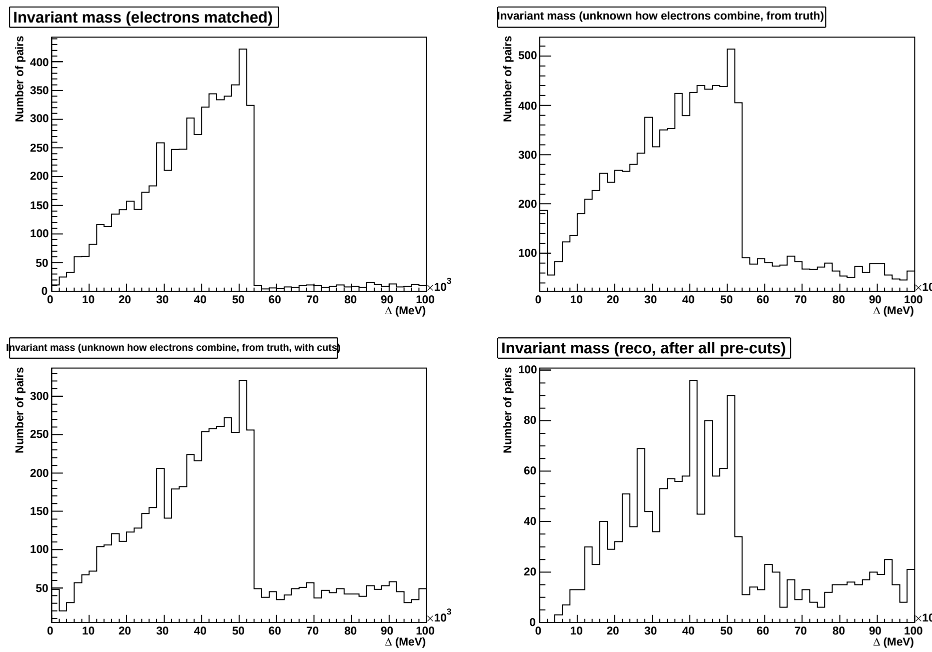

Figure 20: Invariant mass looking solely at signal events. Top left is OSSF electrons when we know how they should be paired using truth parent data. Top right is truth data for combinations of OSSF pairs. Bottom left and bottom right are the reconstructed data, after the pre-cuts, the bottom left prior to any electron cuts, the bottom right with electron cuts.

$\sim$90 events to $\sim$20 events, a much smaller difference than we had previously. The peaks still seem to be in approximately the same place as in our truth studies, so the mass determination should still be accurate.

7.3 Including Standard Model Background

We now add the complication of background data and reproduced our graph of OSSF pairs in figure 21. It is clear that if we look at solely the background such an edge does not occur (right hand figure), while with the signal there is a clear edge again, at the correct value of Δ. Yet again, however, the edge is clear but even smaller than it was previously — going from $\sim$100 events to $\sim$30 events.

7.4 Further Study

The invariant mass section was not the main focus of this project, however we have been able to gain a brief insight into it, and have seen that it should be possible to determine this invariant mass and thus the mass difference between the $\tilde{\chi}_1^0$ and $\tilde{e}_R$. Further work on this area would include removing the combinatorial background, which would help improve the edge resolution and should not be too difficult since the simple assumption that this background is constant should be sufficient. It would also be useful to fit a function to these histograms in order to try and determine what values

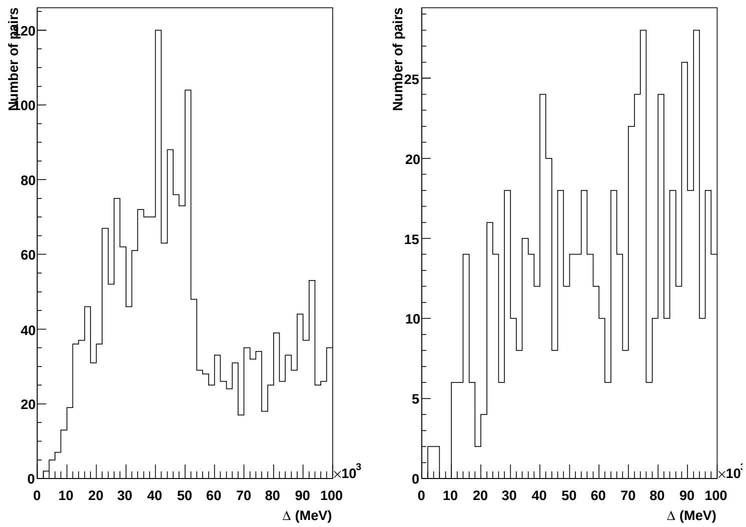

Figure 21: Invariant mass looking solely at signal events with background (on the left) and just background (right).

of the masses these results would give us were they from real experiments, and compare this to the data we put into the Monte Carlo generator.

8 Conclusion

This study set out to investigate the potential for discovery of GMSB4 at ATLAS using electrons. It has been shown that there certainly is discovery potential, and we should even be able to produce very high ratios of signal events to background events by making appropriate cuts, meaning that it could be observed relatively quickly and clearly. These cuts could be even harder on missing transverse energy than the 100 GeV assumed in this report, and this could be combined with a softer jet cuts, which would increase our number of signal events without a correspondingly sized increase in background.

A study of these cuts would need to be performed with a new background sample, since the generator cuts mean than reducing the jet cuts is not viable with this sample. It might also be worth considering including rarer SM processes in the background — events with two Zs or two Ws would be more likely to produce electrons than the background events we would looked at, and it is possible they might also produce more missing E_T. Again, this would require a new set of background samples.

The analysis undertaken here could be repeated for muons, by making appropriate changes, and this is a very useful part of the GMSB4 theory — we should be able to cross-check electron and muon data once the LHC is up and running to investigate it. This could be considered for either the ATLAS or CMS detectors. The analysis of muons should in principle be easier, since muons can be identified very easily and there is a large muon system for both ATLAS and CMS.

In addition to indicating that GMSB4 should be readily discoverable at the LHC, we also now have a better understanding of how the SUSY particles in it behave, particularly at the end of the decay chains. The brief investigation on the SUSY relative mass determination indicates that this can be measurable and precise, and further analysis on this could be considered.

Appendix A : Graphs

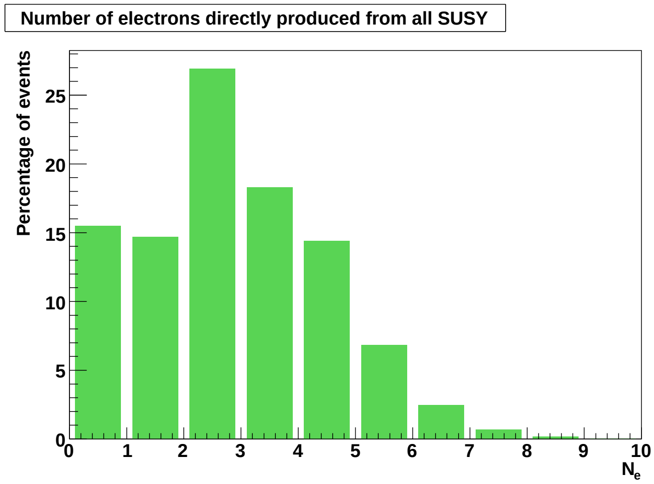

Figure 22: The number of electrons produced from the whole SUSY chain

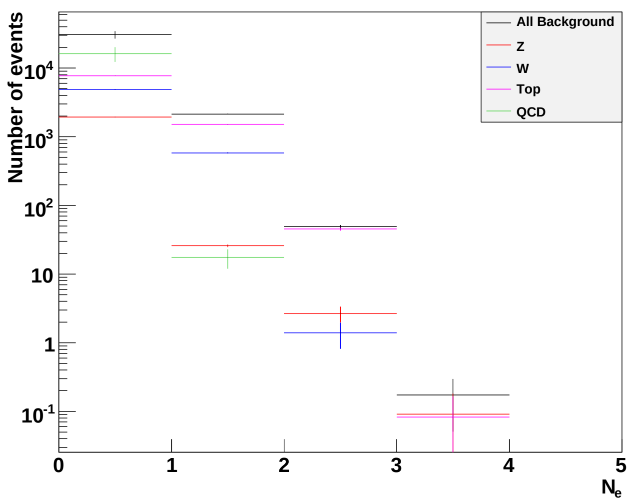

Figure 23: Electron distribution for background events only

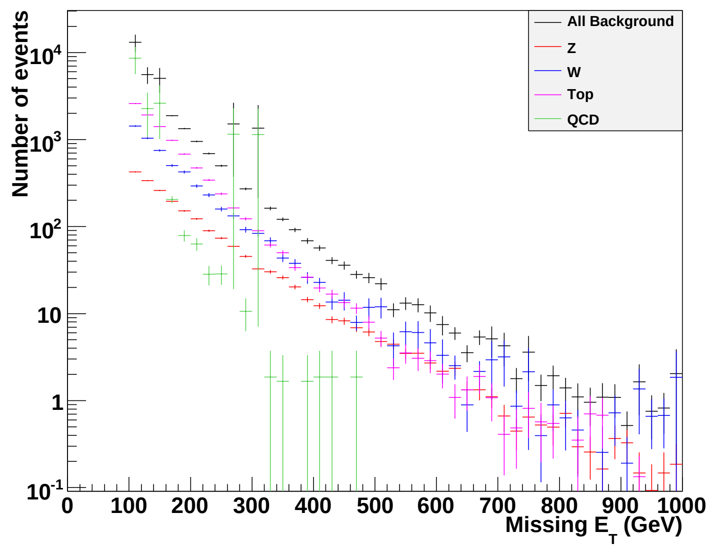

Figure 24: Missing E_T for background events only

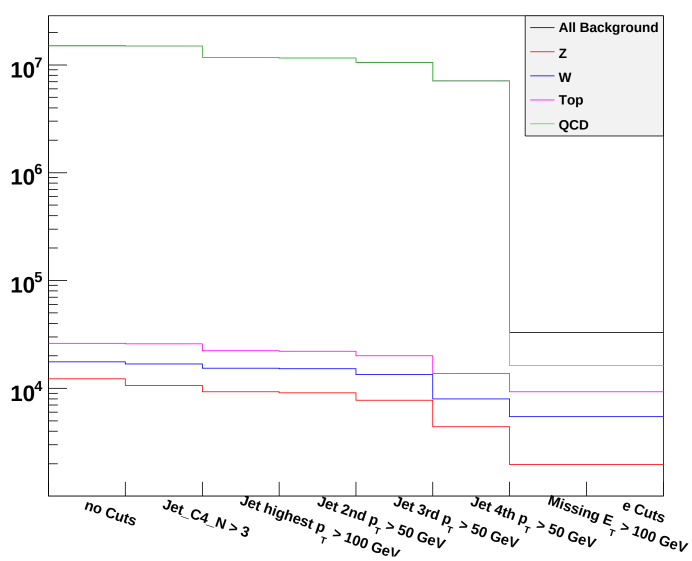

Figure 25: The cut flow diagram for background events only

Appendix B : Invariant Mass Calculation

We are considering the decay $\tilde{\chi}_1^0 \to \tilde{e}_R e^{(1)} \to \tilde{G} e^{(1)} e^{(2)}$. The $^{(1)}, ^{(2)}$ are just labels so we can identify the two electrons.

Considering the decay of the $\tilde{e}_R$ in its own rest frame :

$$m_{\tilde{e}_R} = E_{e^{(2)}} + E_{\tilde{G}} \qquad \mathbf{p}_{e^{(2)}} = -\mathbf{p}_{\tilde{G}}. \tag{1}$$

If we neglect the mass of the electron, we can write the graviton momentum as

$$\begin{aligned} \mathbf{p}_{\tilde{G}}^2 &= E_{\tilde{G}}^2 - m_{\tilde{G}}^2 \\ &= (m_{\tilde{e}_R} - E_{e^{(2)}})^2 - m_{\tilde{G}}^2 \\ &= (m_{\tilde{e}_R} - |\mathbf{p}_{e^{(2)}}|)^2 - m_{\tilde{G}}^2 \\ &= (m_{\tilde{e}_R} - |\mathbf{p}_{e^{(2)}}|)^2 - m_{\tilde{G}}^2 \\ &= m_{\tilde{e}_R}^2 + |\mathbf{p}_{e^{(2)}}|^2 - 2m_{\tilde{e}_R} |\mathbf{p}_{e^{(2)}}| - m_{\tilde{G}}^2. \end{aligned} \tag{2}$$

Using the fact $\mathbf{p}_{e^{(2)}} = -\mathbf{p}_{\tilde{G}}$ gives us

$$\begin{aligned} 2m_{\tilde{e}_R} |\mathbf{p}_{e^{(2)}}| &= m_{\tilde{e}_R}^2 - m_{\tilde{G}}^2 \\ \implies |\mathbf{p}_{e^{(2)}}| &= \frac{m_{\tilde{e}_R}^2 - m_{\tilde{G}}^2}{2m_{\tilde{e}_R}}. \end{aligned} \tag{3}$$

We now consider the decay of the $\tilde{\chi}_1^0$. Again, in the rest frame of the $\tilde{e}_R$:

$$E_{\tilde{\chi}_1^0} = m_{\tilde{e}_R} + E_{e^{(1)}} \qquad \mathbf{p}_{\tilde{\chi}_1^0} = \mathbf{p}_{e^{(1)}}. \tag{4}$$

Again neglecting the mass of the electron, we now write the neutralino momentum as

$$\begin{aligned} \mathbf{p}_{\tilde{\chi}_1^0}^2 &= E_{\tilde{\chi}_1^0}^2 - m_{\tilde{\chi}_1^0}^2 \\ &= (m_{\tilde{e}_R} + E_{e^{(1)}})^2 - m_{\tilde{\chi}_1^0}^2 \\ &= (m_{\tilde{e}_R} + |\mathbf{p}_{e^{(1)}}|)^2 - m_{\tilde{\chi}_1^0}^2 \\ &= (m_{\tilde{e}_R} + |\mathbf{p}_{e^{(1)}}|)^2 - m_{\tilde{\chi}_1^0}^2 \\ &= m_{\tilde{e}_R}^2 + |\mathbf{p}_{e^{(1)}}|^2 + 2m_{\tilde{e}_R} |\mathbf{p}_{e^{(1)}}| - m_{\tilde{\chi}_1^0}^2 \end{aligned} \tag{5}$$

and so, similarly to before

$$\begin{aligned} 2m_{\tilde{e}_R} |\mathbf{p}_{e^{(1)}}| &= m_{\tilde{\chi}_1^0}^2 - m_{\tilde{e}_R}^2 \\ \implies |\mathbf{p}_{e^{(1)}}| &= \frac{m_{\tilde{\chi}_1^0}^2 - m_{\tilde{e}_R}^2}{2m_{\tilde{e}_R}}. \end{aligned} \tag{6}$$

The invariant mass of the electrons, Δ is given by:

$$\begin{aligned} \Delta^2 &= (E_{e^{(1)}} + E_{e^{(2)}})^2 - (\mathbf{p}_{e^{(1)}} + \mathbf{p}_{e^{(2)}})^2 \\ &= E_{e^{(1)}}^2 + E_{e^{(2)}}^2 + 2E_{e^{(1)}} E_{e^{(2)}} - |\mathbf{p}_{e^{(1)}}|^2 - |\mathbf{p}_{e^{(2)}}|^2 - 2\mathbf{p}_{e^{(1)}} \cdot \mathbf{p}_{e^{(2)}} \\ &= 2\,|\mathbf{p}_{e^{(1)}}|\,|\mathbf{p}_{e^{(2)}}| - 2\mathbf{p}_{e^{(1)}} \cdot \mathbf{p}_{e^{(2)}} \\ &= 2\,|\mathbf{p}_{e^{(1)}}|\,|\mathbf{p}_{e^{(2)}}|\,(1 - \cos\theta) \end{aligned} \tag{7}$$

where the third line follows by neglecting electron masses. This is maximal when the angle between the electrons, θ, $= \pi$, and so if we plug in our values for $|\mathbf{p}_{e^{(1)}}|$ and $|\mathbf{p}_{e^{(2)}}|$:

$$\begin{aligned}\Delta^2_{\mathrm{max}} &= \frac{\left(m^2_{\tilde{\chi}^0_1} - m^2_{\tilde{e}_R}\right)\left(m^2_{\tilde{e}_R} - m^2_{\tilde{G}}\right)}{m^2_{\tilde{e}_R}} \\ &= m^2_{\tilde{\chi}^0_1} - m^2_{\tilde{e}_R}\end{aligned} \tag{8}$$

since the gravitino mass is very nearly zero by comparison to the neutralino and selectron.

Acknowledgements

Many thanks to my supervisor Wolfgang Ehrenfeld for his continued help and guidance throughout the project. Mark Terwort and Doëthe Ludwig were also very helpful. Additionally, thanks are due to the whole ATLAS analysis group at DESY and the Summer Student Programme organisers.

References

[1] ATLAS Collaboration. Atlas detector and physics performance : Technical design report, 1999.

[2] ATLAS Collaboration. Studies of SUSY signatures with high-pT photons or long-lived heavy particles in ATLAS, 2008.

[3] Manuel Drees. An introduction to supersymmetry, 1996.

[4] John Ellis. Supersymmetry for ALP hikers, 2002.

[5] C. Amsler *et al.* Review of particle physics. *Phys. Lett. B 667, 1.*, 2008.

[6] G. F. Giudice and R. Rattazzi. Theories with gauge-mediated supersymmetry breaking. *Physics Reports*, 322:419, 1999.

[7] http://en.wikipedia.org/wiki/Pseudo rapidity. Wikipedia : Pseduo-rapidity.

[8] Christopher Kolda. Gauge-mediated supersymmetry breaking: Introduction, review and update. *Nuclear Physics B - Proceedings Supplements*, 62:266, 1998.

[9] Stephen P. Martin. A supersymmetry primer, 1997.

[10] Hitoshi Murayama. Supersymmetry phenomenology, 2000.